**Astronomy
&
Astrophysics**

A likely exoplanet orbiting the oscillating K-giant α Arietis[*]

B.-C. Lee[1], D. E. Mkrtichian[2], I. Han[1], K.-M. Kim[1], and M.-G. Park[3]

[1] Korea Astronomy and Space Science Institute, 776, Daedeokdae-Ro, Youseong-Gu, 305-348 Daejeon, Korea
e-mail: [bclee;iwhan;kmkim]@kasi.re.kr
[2] Crimean Astrophysical Observatory, Nauchny, 98409 Crimea, Ukraine
e-mail: davidm@crao.crimea.ua
[3] Department of Astronomy and Atmospheric Sciences, Kyungpook National University, 702-701 Daegu, Korea
e-mail: mgp@knu.ac.kr

ABSTRACT

Aims. To search for extrasolar planets around intermediate-mass stars, we are conducting a precise RV survey around K-giants.
Methods. We present high-accuracy RV measurements of α Ari made from November 2003 to February 2010. This star belongs to our sample of 55 K-giants studied for extrasolar planet and pulsation searches using the fiber-fed Bohyunsan Observatory Echelle Spectrograph (BOES) attached to the 1.8-m telescope at Bohyunsan Optical Astronomy Observatory (BOAO) in Korea.
Results. We find a planetary companion with long-period and low-amplitude radial velocity (RV) variations in oscillating K2 III star α Ari (HD 12929). We do not find the correlation between RV variations and chromospheric activity indicators (Ca II H & K region, Hα line). The bisector analysis also shows that the bisector velocity span (BVS) does not show any obvious correlation with RV variation but has periodic component that may be attributed to the rotation of the star. If the RV variation is indeed caused by a planetary companion, an orbital solution with a period of $P = 381$ days, a semi-amplitude of $K = 41$ m s^{-1}, and an eccentricity of $e = 0.25$ fits the data best. Assuming a possible stellar mass of $M_\star = 1.5\ M_\odot$, we estimate the minimum mass for the planetary companion of $m_2 \sin i = 1.8\ M_{\rm Jup}$ with an orbital semi-major axis of 1.2 AU.
Conclusions. Our finding of a likely exoplanet in α Ari supports searching for extrasolar planets around giant stars with multiperiodic oscillations.

Key words. planetary systems – stars: individual: α Arietis – techniques: radial velocities

1. Introduction

Ever since the first extrasolar planet around a main-sequence star was discovered by Mayor & Queloz (1995), about 500 extrasolar planets have been found so far. Most of them are found around main-sequence stars using the precise RV method, but several planets have only been found around giant stars.

Detection around intermediate-mass stars evolving toward the giant stage is easier than around early stage or main-sequence stars thanks to the availability of many sharp absorption lines for high-precision RV measurements. This makes giant stars suitable targets for extrasolar planet detection with the RV method. Frink et al. (2002) discovered the first planetary companion around the K-giant star ι Dra (K2 III), and thereafter, several companions around K-giant stars have been reported using the precise RV method (Setiawan 2003; Setiawan et al. 2003; Mitchell et al. 1234; Hatzes et al. 2005, 2006; Reffert et al. 2006; Johnson et al. 2007, 2008; Döllinger et al. 2007, 2009; de Medrios et al. 2009; and Sato et al. 2007, 2008a,b, 2010). However, in K-giants the velocity variations caused by planetary companions can be blended with the stellar pulsations and surface activities, which complicates identification of planetary companions.

K-giant α Ari (HD 12929, HR 617) is one of our sample 55 K-giant stars for which we have obtained precise

RV measurements in the past eight years at BOAO in Korea. In previous publication, we (Kim et al. 2006) reported multiperiodic oscillations in α Ari with periods $P_1 = 0.571$ day (or aliases at 0.445 or 0.871 days) observed during November to December 2003. The average amplitude variation ranges $\sim\pm20$ m s^{-1} just overnight. This variability can only be the result of stellar oscillations because of the short time scale. We continued to observe α Ari, by getting several spectra every night to search for long-term variation. Here we report the detection of a long-period and low-amplitude RV variation of α Ari possibly due to a planetary companion.

2. Observations and analysis

We acquired 678 spectra of α Ari from November 2003 to February 2010 using the fiber-fed high resolution ($R = 90\,000$ at 5000 Å) echelle spectrograph BOES (Kim et al. 2007) attached to the 1.8-m telescope at BOAO in Korea. An iodine absorption cell (I$_2$) was used to provide the precise RV measurements. Each estimated signal-to-noise ratio (S/N) at I$_2$ wavelength region is about 250 with typical exposure time ranging between 90 and 180 s.

The extraction of normalized 1–D spectra was carried out using IRAF (Tody 1986) software. Further data processing, I$_2$ analysis and precise RV measurements were undertaken using a code called RVI2CELL (Han et al. 2007) developed at the Korea Astronomy & Space Science Institute (KASI).
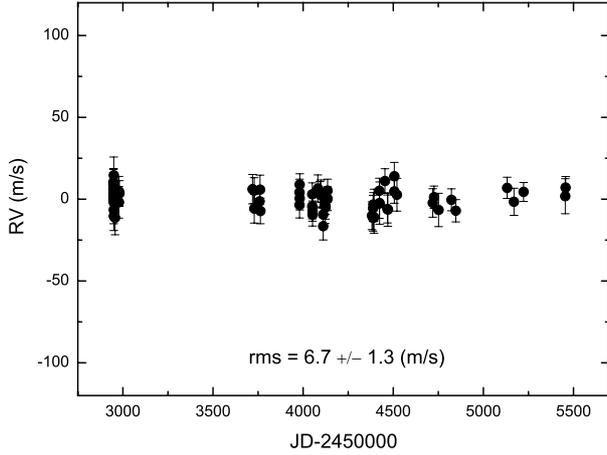
To demonstrate a long-term stability of the BOES we show relative RV measurements of the standard star τ Ceti in Fig. 1. It shows that RV of τ Ceti is constant with an rms scatter of $6.7 \, \mathrm{m\,s^{-1}}$, over the time span of our observations.

3. The properties of α Ari

We refer to the main photometric parameters of α Ari to Allende Prieto & Lambert (1999) taken from the Hipparcos catalogs of stars within 100 pc from the Sun and the main spectroscopic parameters to Hekker & Meléndez (2007) taken at Lick observatory.

The mean RV of α Ari is $-14.6 \, \mathrm{km\,s^{-1}}$ (Evans 1967). Berdyugina et al. (1991) derived $T_{\mathrm{eff}} = 4850 \pm 150$ K. And, Gray et al. (2002) determined $T_{\mathrm{eff}} = 4481 \pm 11$ K and [Fe/H] = -0.221 ± 0.036. Mozurkewich et al. (1991) measured an angular diameter for α Ari of 6.412 ± 0.064 mas at 800 nm. The Hipparcos parallax of 49.48 ± 0.99 mas results in a stellar radius of $13.9 \pm 0.3 \, R_\odot$. The most recent determinations of the projected rotational velocity $v_{\mathrm{rot}} \sin i = 3.44 \, \mathrm{km\,s^{-1}}$ by Hekker & Meléndez (2007) and $3.1 \pm 1 \, \mathrm{km\,s^{-1}}$ by Carney et al. (2008) are close to each other. Based on the latter value that is given with error estimation, we derived the range of upper limit for the rotational period of

$$P_{rot} = 2\pi R/(v_{\mathrm{rot}} \sin i) = 172{-}335 \text{ days}.$$

Berdyugina et al. (1991) determined $\log g = 2.6 \pm 0.3$, almost in agreement with $\log g = 2.57 \pm 0.2$ as determined by McWilliam (1990). Surface gravity and its uncertainty $\log g = 2.6 \pm 0.3$ yields a stellar mass in the range of $1.4{-}5.6 \, M_\odot$. To estimate the mass of α Ari independently, we determined atmospheric parameters directly from our spectra. By using measured 268 equivalent widths (EW) of Fe I and Fe II lines, we estimated T_{eff}, [Fe/H] = -0.09 ± 0.03, $\log g$, and v_{micro} of the star using the program TGVIT (Takeda et al. 2005). Our estimated surface gravity with its formal uncertainty is $\log g = 2.33 \pm 0.06$. That yields a stellar mass of $1.5 \pm 0.2 \, M_\odot$. Table 1 summarizes the basic stellar parameters of α Ari.

4. Orbital solution

The long-term variation of α Ari was first noted by Walker et al. (1989) and Larson et al. (1999) who used CFHT 3.6-m and DAO telescopes with a hydrogen-fluoride (HF) absorption

Table 1. Stellar parameters for α Ari.

Parameter	Value	Reference
Spectral type	K2 III	Hekker & Meléndez (2007)
m_v [mag]	2.01	Hipparcos
M_v [mag]	0.48 ± 0.09	Hipparcos
$B - V$ [mag]	1.151	Hipparcos
Parallax [mas]	49.48 ± 0.99	Hipparcos
Diameter [mas]	6.412 ± 0.064	Hipparcos
Distance [pc]	20.2	Hipparcos
RV [km s^{-1}]	-14.6 ± 0.1	Evans (1967)
T_{eff} [K]	4480	McWilliam (1990)
	4850 ± 150	Berdyugina et al. (1991)
	4481 ± 11	Gray et al. (2002)
	4553 ± 15	This work
[Fe/H]	-0.25	McWilliam (1990)
	-0.22	Mozurkewich et al. (1991)
	-0.09 ± 0.03	This work
$\log g$	2.57 ± 0.2	McWilliam (1990)
	2.6 ± 0.3	Berdyugina et al. (1991)
	2.33 ± 0.06	This work
$M_\star$ [$M_\odot$]	1.5 ± 0.2	This work
$R_\star$ [$R_\odot$]	13.9 ± 0.3	derived
$v_{\mathrm{rot}} \sin i$ [km s^{-1}]	3.44	Hekker & Meléndez (2007)
	3.1 ± 1	Carney et al. (2008)
$P_{\mathrm{rot}}/\sin i$ [days]	172–335	derived
v_{micro} [km s^{-1}]	1.7	McWilliam (1990)
	1.40 ± 0.06	This work

cell. These data were insufficient (45 spectra) to draw any conclusions about possible periodic variability. We recalculated the standard deviation of their 45 measurements of RV variation of $\sigma_{\mathrm{CFHT}} = 41.6 \pm 6.2 \, \mathrm{m\,s^{-1}}$ during 13 years. The standard deviation of our 678 measurements spanning eight years is $\sigma_{\mathrm{BOAO}} = 27.1 \pm 1.6 \, \mathrm{m\,s^{-1}}$.
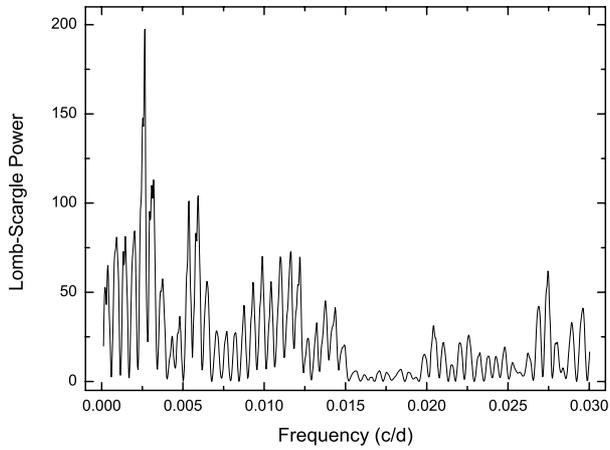
Figure 3 shows the Lomb-Scargle periodogram (Lomb 1976; Scargle 1982) of the original RV time series for α Ari. It shows a significant power at $f_1 = 0.00263 \, \mathrm{c\,d^{-1}}$ ($P = 380.8$ days). The individual RV measurements are shown on the top panel in Fig. 2, and they exhibit clear variations.

The statistical significance of this signal was calculated using the bootstrap randomization technique (e.g. Hatzes & Mkrtichian 2004, and references herein). The measured RV values were randomly shuffled keeping the observed times fixed. The Lomb-Scargle periodogram was then computed 200 000 times for each "random" data set. The fraction of a periodogram having power higher than the amplitude peak in the range of $0 < f < 0.03 \, \mathrm{c\,d^{-1}}$ represents the false-alarm probability (FAP) that noise would create the detected signal. A small FAP is therefore an indication of a significant peak. We found that among 200 000 trials the highest peak of periodograms never exceed a signal in the original data, thus the FAP $< 5 \times 10^{-6}$.

The solid line in the top panel of Fig. 2 is the best-fit Keplerian orbit with $P = 380.8 \pm 0.3$ days, semi-amplitude $K = 41.1 \pm 0.8 \, \mathrm{m\,s^{-1}}$ and eccentricity of 0.25 ± 0.03. We estimated the minimum mass of the companion to be $1.8 \pm 0.2 \, M_{\mathrm{Jup}}$ at a distance of 1.2 AU from α Ari. The RV phase diagram for the orbit in Fig. 2 is shown in Fig. 4. CFHT data (open circles) are also shown in the phase diagram to the period of BOES data set. Uncertainties of CFHT RV measurements are $2 \sim 3$ times larger than that of BOES and also do not conform perfectly with BOES phase diagram because of low instrumental exquisiteness and some noise pattern of the data (Larson et al. 1993, 1999). The rms residual from the orbital solution is $17.8 \, \mathrm{m\,s^{-1}}$ (Fig. 2).
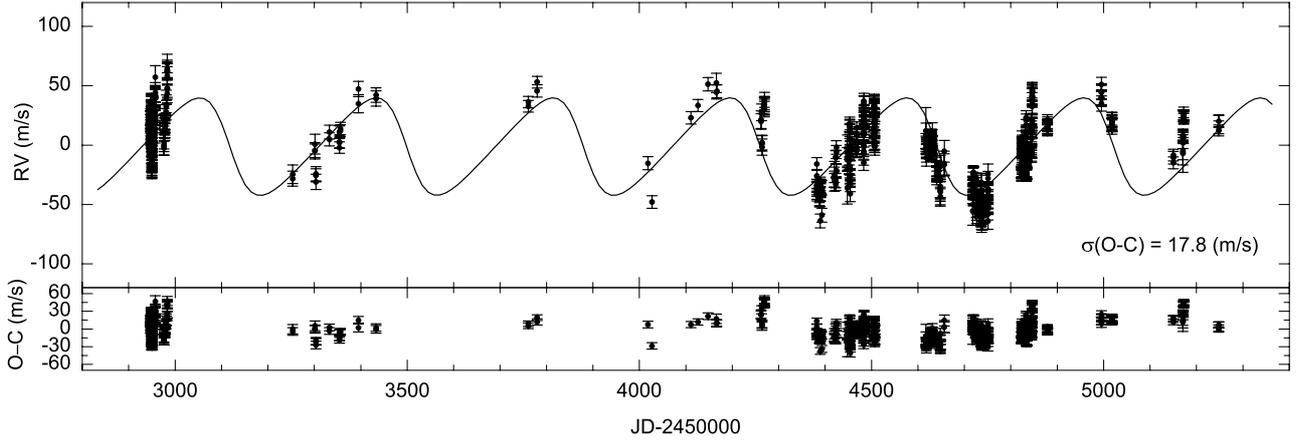
Fig. 2. RV measurements (*top*) and rms scatter of the residuals (*bottom*) for α Ari taken at BOAO from November 2003 to February 2010. The solid line is the orbital solution with a period of 380.8 days and an eccentricity of 0.25.

Fig. 3. The Lomb-Scargle periodogram of the RV measurements for α Ari. The periogram shows a significant power at a frequency of 0.00263 c d^{-1} corresponding to a period of 380.8 days.
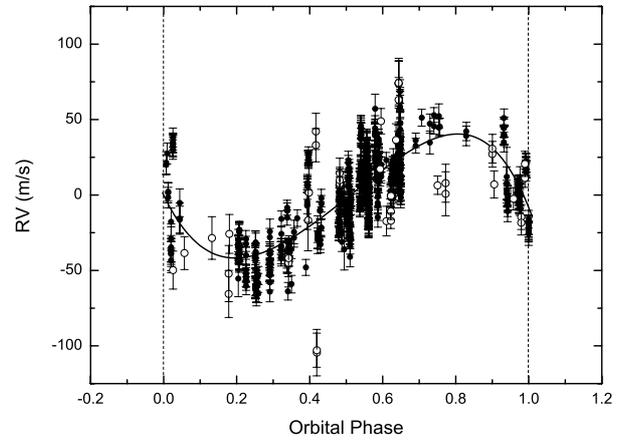
Fig. 4. RVs of α Ari phased to the period of 380.8 days. Filled and open circles denote BOES and CFHT spectroscopic measurements, respectively. The solid line is the orbital solution that fits the data with an rms of 17.8 m s^{-1}.

This is almost certainly due to the short-period variations and intrinsic variability of stellar oscillations, as shown by Kim et al. (2006). All the orbital elements are listed in Table 2.

5. The nature of the RV variations

K-giant stars exhibit pulsation, as well as surface activity, resulting in low-amplitude RV variability on different time scales. While short-term period (hours $\sim$ days) RV variations have been known to be the result of stellar pulsations (Hatzes & Cochran 1998), long-term period (a hundred of days) RV variations with a low-amplitude may be caused by three kinds of phenomena: planetary companion, rotational modulation of surface features, or non-radial oscillation modes. To establish whether a low amplitude and long-period RV variations are caused by surface activities or companions we examined: 1) the Hipparcos photometry, 2) the stellar chromospheric activity indicators like the EW of sensitive lines, and 3) spectral line bisectors measurement.
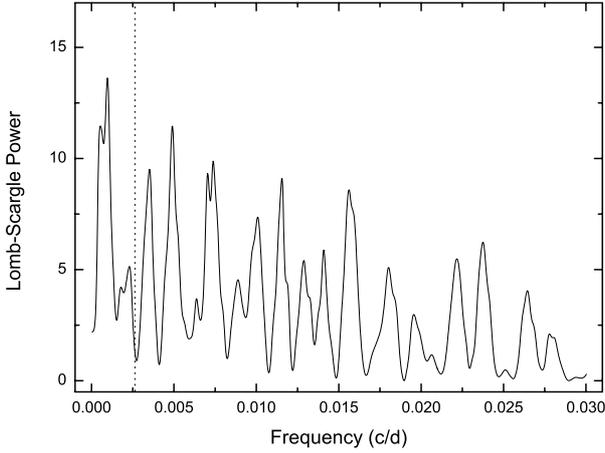
5.1. Hipparcos photometry

We analyzed the Hipparcos photometry for α Ari in order to search for possible brightness variations due to the rotational modulation of cool surface spots in case the RV variation is

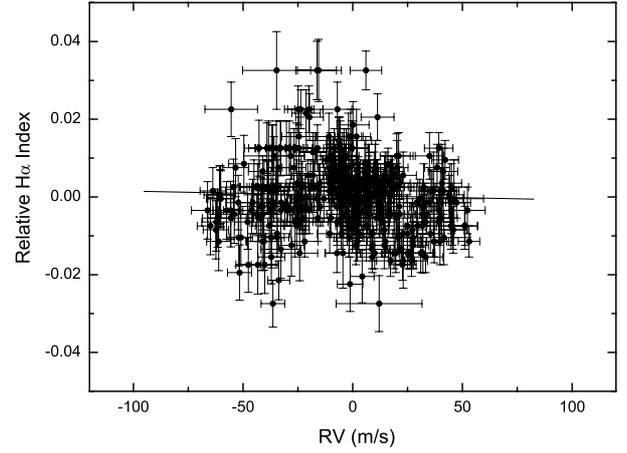**Table 2.** Orbital parameters of the RV measurements for α Ari b.

Parameter	Value
Period [days]	380.8 ± 0.3
$T_{\text{periastron}}$ [JD]	$2\,451\,213.52 \pm 7.36$
K [m s^{-1}]	41.1 ± 0.8
e	0.25 ± 0.03
ω [deg]	89.16 ± 6.84
$f(m)$ [$M_\odot$]	$(2.476) \times 10^{-9}$
$m \sin i$ [M_{Jup}]	1.8 ± 0.2
a [AU]	1.2
σ (O–C) [m s^{-1}]	17.8

caused by the rotation. For 2.5 years, the Hipparcos satellite obtained 66 photometric measurements of α Ari, and we used the whole data except one measurement with a large error.
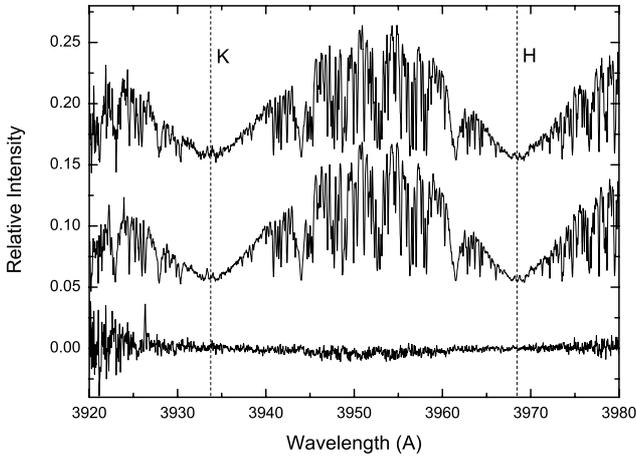
Figure 5 shows the Lomb-Scargle periodogram of Hipparcos photometric measurements calculated in the frequency interval of 0–0.03 c d^{-1}. There are no significant peaks near the frequency of $f_1 = 0.00263$ c d^{-1} that corresponds to the period of 381 days. Peaks in the periodogram are the typical low-frequency noise peaks so they cannot be considered as significant.

Fig. 6. The spectral region of the Ca II H & K lines in α Ari. Two spectra exhibiting the positive (*top*) and the negative (*middle*) RV deviations are displayed (see text). *Bottom* shows the differential spectrum. Any systematic difference in line profiles and core reversals are not apparent around the Ca II H & K central region, indicating modest activity.

5.2. Chromospheric activity indicators

The EW variations of Ca II H & K, H_α, and Ca II 6882 Å lines are frequently used for chromospheric activity analysis. The emissions in the Ca II H & K core are formed in the chromosphere and show a typical central reversal in the existence of chromospheric activity (Pasquini et al. 1988; Saar & Donahue 1997). Because the Ca II H & K line region of the BOES spectra does not have enough S/Ns to estimate EW variations of each spectrum reliably, we used the averaged Ca II H & K line profiles at the upper and lower part of RV curve to see any systematic difference related to the RV variations. We selected spectra for α Ari that correspond to the positive deviation on JD-2 453 779.9451 (RV = 52.9 m s^{-1}) and the negative deviation on JD-2 454 027.1307 (RV = –48.1 m s^{-1}) of RV curve. These spectra in the Ca II H & K region were plotted in Fig. 6. Core reversal in the Ca II H & K central region is not obvious and there is no systematic difference in the line profiles at these two extremal parts of the RV curve. It means that K-giant α Ari, at the moment of observations, exhibits a modest chromospheric activity.

Fig. 7. Relative EW(Å) vs. RV of the H_α line for α Ari from September 2004 to February 2010. The diagram shows no correlation between the EWs and the RVs.

The Balmer H_α line can also be a useful indicator of chromospheric activity to determine whether the RV variation is due to intrinsic stellar variability (Kürster et al. 2003). Unlike in main sequence stars where H_α line is blended with telluric and broad lines, it is easy to measure the EW of H_α line in giant stars. The mean EW of the H_α line in α Ari is measured to be 1087.5 ± 9.1 mÅ. The rms of 9.1 mÅ corresponds to a 0.84% variation in the EW. Figure 7 shows the EW of the H_α line as a function of RV. A gradual slope (solid line) of the fitted line shows that the EWs of the H_α line are not correlated with RV variations.

We conclude that the chromospheric activity and surface spots, if present, have too small amplitude to be resolved in the Ca II H & K and the H_α line EW variations. Another activity indicator Ca II 8662 Å line is not suitable because the significant fringing and saturation of our CCD spectra at wavelengths are longer than 7500 Å.

5.3. Line bisector variations

Queloz et al. (2001) report that the analysis of the line bisector can distinguish the origin of the observed RV variations, which is very useful for the messy K-giant stars. The RV variations due to planetary companions should not produce any changes in the spectral line shape, whereas the surface inhomogeneities do. Stellar rotation modulations of surface features can create variable asymmetries in the spectral line profiles. Thus, the analysis of the shapes of spectral lines may prove or disprove the existence of planetary companions.

Bisector velocity span (BVS) is defined as the difference between two regions of the bisector at the top and bottom of the profile to measure changes with high accuracy. To search for variations in the spectral line shapes, we measured the BVS using the mean profile of the spectral lines. We calculated the mean profile of spectral lines using the least squares deconvolution (LSD) technique (Glazunova et al. 2008). We used the Vienna Atomic Line Database (VALD; Piskunov et al. 1995) to prepare the list of spectral lines. The total of 4339 lines within the wavelength region of 4500–4900 and 6450–6840 Å were used to construct the LSD profile, which excluded spectral regions around the I_2 absorption region, hydrogen lines, and regions with strong contamination by terrestrial atmospheric lines. We estimated the BVS of the mean profile between two different flux levels of central depth levels 0.8 and 0.25 as the span points.
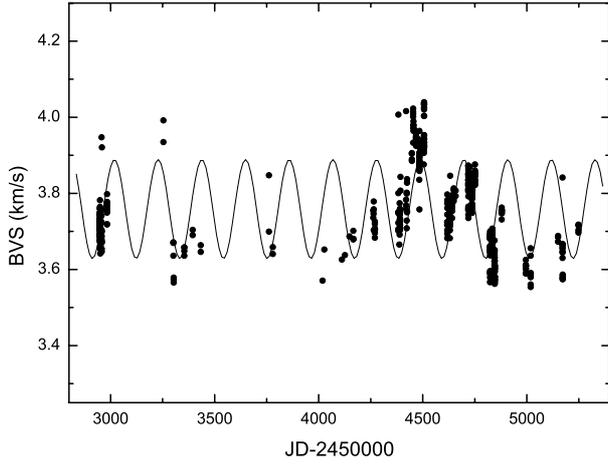
Fig. 8. BVS variations for α Ari from November 2003 to February 2010. The solid line shows a sine wave with a period of 211 days fit.

The BVS vs. JD shown in Figure 8 exhibits some periodic variations. The BVSs of the JD 2 454 453–2 454 506 spectra seem to be shifted with respect to the preceding and subsequent data by the amount grater than the $+100$ m s^{-1}. We suspect that this bias was come from the temporary mis-alignments of the BOES echelle spectrometer. But, we did not find any BVS shift in the K-giant γ^1 Leo for the same observing epoch as where a planetary companion system was detected by using the same echelle spectrometer BOES (Han et al. 2010). The RV code RVI2CELL takes any changes into account in the instrumental profile in calculations of RVs, and thus instrumental misalignment is not likely to have affected the RV data.

To search for periodic signals in the BVS data we calculated the Lomb-Scargle periodogram of the BVS (top panel in Fig. 9). The largest peak in the Lomb-Scargle periodogram is at a very low frequency, $f_1 = 0.00108$ c d^{-1} ($P = 926.8$ days) with an FAP less than 9×10^{-6}. After removal of this signal, we plot the Lomb-Scargle periodogram of the residuals at bottom panel in Fig. 9. The highest peak at $f_2 = 0.00474$ c d^{-1} ($P = 211.2$ days) has high FAP $\sim 2 \times 10^{-5}$. Figure 8 shows the individual fit of the frequency to BVS data.

Taking the stellar radius and rotational velocity ($v_{\rm rot} \sin i$) value into account we derived the expected range of rotational period of 172–335 days. Found about 211 day periods of BVS variations well fit this interval. We can summarize that the variation can be attributed to stellar surface active regions, inhomogeneities, and rotation.

6. Discussion and conclusion

Our analysis of the RV measurements for α Ari revealed a 381 day periodic variation that persisted between 2003–2010 for almost six cycles with no changes in phase or amplitude. We also confirmed the short-period oscillations previously found in α Ari (Kim et al. 2006). We found no evidence of the correlation between the 381 day RV variation and the EWs of H$_\alpha$ lines or the Hipparcos photometry. But, we found about 211 day periodic variations in the BVS that we attribute to the rotational modulation of line profiles from the surface spots and about 927 day variations in the unknown origin. Thus, we conclude that the planetary companion in α Ari is the most likely cause of the 381 day RV variations.

If confirmed, the determined orbit of the 1.8 $M_{\rm Jup}$ mass planet is fairly eccentric, $e = 0.25 \pm 0.03$, but, up to now,
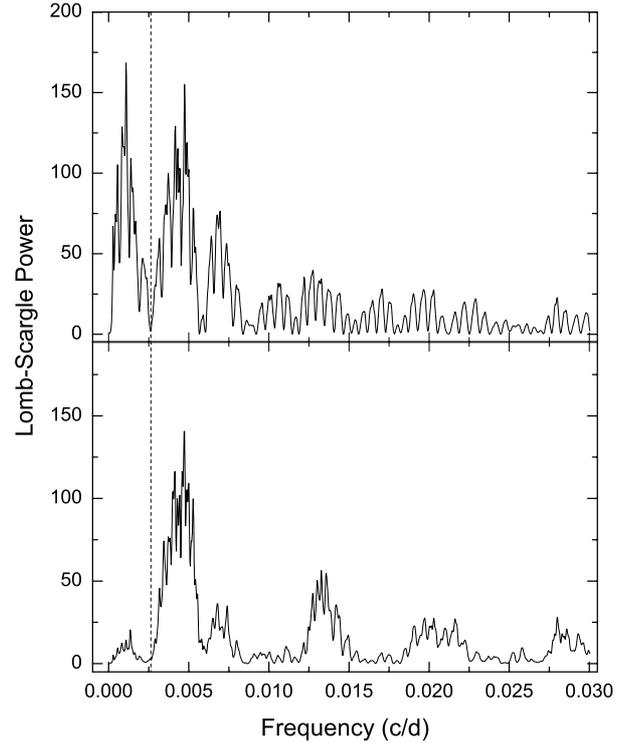
Fig. 9. The Lomb-Scargle periodogram of the BVS variations from November 2003 to February 2010 (*top panel*) and after subtracting the low-frequency ($f_1 = 0.00108$ c d^{-1}) variations (*bottom panel*). The highest frequency is at $f_2 = 0.00474$ c d^{-1} ($P = 211.2$ days). The vertical dotted line marks the location of the orbital frequency.

6 out of 22 companions around K-giants show more than 0.2 eccentricity: $e = 0.7$ of ι Dra (Frink et al. 2002), $e = 0.2$ of K1 III star HD 47536 (Setiawan et al. 2003,b), $e = 0.27$ of K1 II-III star HD 13189 (Hatzes et al. 2005), $e = 0.43$ of K1 III star 4 UMa (Döllinger et al. 2007), $e = 0.38$ of K1.5 III star 42 Dra (Döllinger et al. 2009), and $e = 0.46$ of K2 III star HD 110014 (de Medeiros et al. 2009). The eccentricity for the planetary orbit of α Ari is therefore not unusual among K-giants, and such eccentric modulation is difficult to produce by surface variations or stellar oscillations.

The source α Ari belongs to yet smaller group of planet hosting K-giants showing short-period oscillations (e.g. β Gem, Hatzes & Zechmeister 2007; ι Dra, Zechmeister et al. 2008).

References

Allende Prieto, C., & Lambert, D. L. 1999, A&A, 352, 555
Berdyugina, S. V., Boyarchuk, M. E., Pavlenko, Y. V., et al. 1991, SvA, 35, 387
Carney, B. W., Gray, D. F., Yong, D., et al. 2008, AJ, 135, 892
Deeming, T. J. 1975, Ap&SS, 36, 137
de Medeiros, J. R., Setiawan, J., Hatzes, A. P., et al. 2009, A&A, 504, 617
Döllinger, M. P., Hatzes, A. P., Pasquini, L., et al. 2007, A&A, 472, 649
Döllinger, M. P., Hatzes, A. P., Pasquini, L., et al. 2009, A&A, 499, 935
Evans, D. S. 1967, IAUS, 30, 57
Frink, S., Mitchell, D. S., Quirrenbach, A., et al. 2002, ApJ, 576, 478
Glazunova, L. V., Yushchenko, A.V., Tsymbal, V. V., et al. 2008, AJ, 136, 1736
Gray, D. F., Scott, H. R., & Postma, J. E. 2002, PASP, 114, 536
Han, I., Kim, K.-M., Lee, Byeong-Cheol, et al. 2007, Publ. Korean Astron. Soc., 22, 75

Han, I., Lee, B. C., Kim, K. M., et al. 2010, A&A, 509, A24
Hatzes, A. P., & Cochran, W. D. 1998, PASPC, 154, 311
Hatzes, A. P., & Mkrtichian, D. E. 2004, MNRAS, 351, 663
Hatzes, A. P., & Zechmeister, M. 2007, ApJ, 670, L37
Hatzes, A. P., Guenther, E. W., Endl, M., et al. 2005, A&A, 437, 743
Hatzes, A. P., Cochran, W. D., Endl, M., et al. 2006, A&A, 457, 335
Hekker, S., & Meléndez, J. 2007, A&A, 475, 1003
Johnson, J. A., Fischer, D. A., Marcy, G. W., et al. 2007, ApJ, 665, 785
Johnson, J. A., Marcy, G. W., Fischer, D. A., et al. 2008, ApJ, 675, 784
Kim, K. M., Mkrtichian, D. E., Lee, B.-C., et al. 2006, A&A, 454, 839
Kim, K.-M., Han, I., Valyavin, G. G., et al. 2007, PASP, 119, 1052
Kürster, M., Endl, M., Rouesnel, F., et al. 2003, A&A, 403, 1077
Larson, A. M., Irwin, A. W., Yang, S. L. S., et al. 1993, PASP, 105, 825
Larson, A. M., Yang, S. L. S., & Walker, G. A. H. 1999, Precise Stellar Radial
    Velocities, IAU Colloq., 170, 185, 193
Lomb, N. R. 1976, Ap&SS, 39, 447
Mayor, M., & Queloz, D. 1995, Nature, 378, 355
McWilliam, A. 1990, ApJS, 74, 1075
Mitchell, D. S., Frink, S., Quirrenbach, A., et al. 2003, BAAS, 35, 1234
Mozurkewich, D., Johnston, K. J., Simon, R. S., et al. 1991, AJ, 101, 2207
Pasquini, L., Pallavicini, R., & Pakull, M. 1988, A&A, 191, 253
Piskunov, N. E., Kupka, F., Ryabchikova, T. A., et al. 1995, A&AS, 112, 525
Queloz, D., Henry, G. W., Sivan, J. P., et al. 2001, A&A, 379, 279
Reffert, S., Quirrenbach, A., Mitchell, D. S., et al. 2006, ApJ, 652, 661
Reiners, A., & Royer, F. 2004, A&A, 428, 199
Saar, S. H., & Donahue, R. A. 1997, ApJ, 485, 319
Sato, B., Izumiura, H., Toyota, E., et al. 2007, ApJ, 661, 527
Sato, B., Izumiura, H., Toyota, E., et al. 2008a, PASJ, 60, 539
Sato, B., Toyota, E., Omiya, M., et al. 2008b, PASJ, 60, 1317
Sato, B., Omiya, M., Liu, Y., et al. 2010, PASJ, 62, 1063
Scargle, J. D. 1982, ApJ, 263, 835
Setiawan, J. 2003, Earths: DARWIN/TPF and the Search for Extrasolar
    Terrestrial Planets, 539, 595
Setiawan, J., Hatzes, A. P., von der Lühe, O., et al. 2003, A&A, 398, L19
Takeda, Y., Ohkubo, M., Sato, B., et al. 2005, PASJ, 57, 27
Tody, D. 1986, Proc. SPIE, 627, 733
Walker, G. A. H., Yang, S., Campbell, B., et al. 1989, ApJ, 343, L21
Zechmeister, M., Reffert, S., Hatzes, A. P., et al. 2008, A&A, 491, 531